Unravelling vascular tumors : combining molecular and computational biology

IJzendoorn, D.G.P. van

Part I

Diagnosis and treatment

Chapter 3

Fusion events lead to truncation of FOS in epithelioid hemangioma of bone

This chapter is based on the publication: **van IJzendoorn DGP**, de Jong D, Romagosa C, Picci P, Benassi MS, Gambarotti M, Daugaard S, van de Sande M, Szuhai K, Bovée JVMG. Fusion events lead to truncation of FOS in epithelioid hemangioma of bone. *Genes Chromosom Cancer*. 2015;54: 565-574.

3.1 Abstract

Epithelioid hemangioma of bone is a locally aggressive vascular neoplasm. It can be challenging to diagnose because of the wide histological spectrum, which can make it difficult to differentiate from other vascular neoplasms such as epithelioid hemangioendothelioma or epithelioid angiosarcoma. COBRA-FISH karyotyping identified a balanced t(3;14) translocation. Transcriptome sequencing of the index case and two other epithelioid hemangiomas revealed a recurrent translocation breakpoint involving the FOS gene, which was fused to different partners in all three cases. The break was observed in exon 4 of the *FOS* gene and the fusion event led to the introduction of a stop codon. In all instances, the truncation of the *FOS* gene would result in the loss of the transactivation domain (TAD). Using FISH probes, we found a break in the *FOS* gene in two additional cases, in none of these cases a recurrent fusion partner could be identified. In total, *FOS* was split in 5/7 evaluable samples. We did not observe point mutations leading to early stop codons in any of the 10 cases where RNA was available. Detection of *FOS* rearrangement may be a useful diagnostic tool to assist in the often-difficult differential diagnosis of vascular tumors of bone. Our data suggest that the translocation causes truncation of the FOS protein, with loss of the TAD, which is thereby a novel mechanism involved in tumorigenesis.

3.2 Introduction

Epithelioid hemangioma of bone (previously known as angiolymphoid hyperplasia with eosinophilia or histiocytoid hemangioma) is a locally aggressive neoplasm composed of cells that have an endothelial phenotype and epithelioid morphology (1). Tumors usually involve long tubular bones (40%), distal lower extremities (18%), flat bones, (18%), vertebrae (16%), and small bones of the hands (8%) (1, 2). It is slightly more common in males and occurs at an average age of 35 years (3). Approximately 18-25% of the tumors display multifocal regional spread (2, 4). The tumors have a lobular architecture, and consist of epithelioid endothelial cells that form vascular lumina or grow in solid sheets (1). The diagnosis of epithelioid hemangioma is challenging, and distinction from epithelioid angiosarcoma can sometimes be difficult (4). Treatment with curettage or marginal en bloc excision is sufficient in most cases, although the tumor can show locally aggressive growth and rare lymph node involvement (2).

The classification of vascular tumors of bone has been controversial, and different classification systems have been proposed over the years (5). They include a heterogeneous group ranging from benign to malignant tumors, including hemangioma, epithelioid hemangioma, epithelioid hemangioendothelioma, and epithelioid angiosarcoma. Part of the

controversy in literature is caused by the fact that cases reported in the past as "hemangioendothelioma of bone" (6–10) probably reflect epithelioid hemangiomas (2, 5, 11), a term which is now generally accepted (1). The new classification of vascular tumors of bone as proposed in the 2013 WHO is supported by the rapid elucidation of novel, characteristic translocations in the different entities. Epithelioid hemangioendothelioma was shown to contain *WWTR1-CAMTA1* or, more rarely, *YAP1-TFE3* fusions (12–14). Recently, a *ZFP36-FOSB* fusion was identified in a subset of epithelioid hemangiomas with atypical features (15). In this study, we used molecular karyotyping to characterize classic epithelioid hemangioma of bone, followed by next generation sequencing analysis. Using COBRA-FISH a balanced translocation t(3;14) was found and by breakpoint mapping using Bacterial Artificial Chromosomes (BAC) clones the approximate locations of the translocation breakpoints were identified. Using transcriptome sequencing, a chimeric sequence was found resulting in a *FOS-MBNL1* fusion gene, as well as fusions involving FOS rearranged with different partner genes in two additional cases. In all three cases, the fusion led to a truncated form of FOS due to early termination of translation. Additional cases were analyzed by interphase FISH probes flanking the *FOS* locus.

3.3 Materials and methods

3.3.1 Patient samples

Eleven epithelioid hemangiomas of bone were available (table 3.1). Cases were acquired from the archives of the Leiden University Medical Center (LUMC), Leiden, The Netherlands, Rizzoli Institute Laboratory of Oncologic Research, Bologna, Italy, and the Department of Pathology, University of Copenhagen, Denmark. Two of the cases from the LUMC showed multifocal regional spread and for all these cases frozen and FFPE material was available from multiple foci (figure 3.1).

For all cases histology was reviewed by two pathologists (JVMGB, CR) and the diagnosis of epithelioid hemangioma was confirmed (table 3.1). All samples were handled according to the Dutch code of proper secondary use of human material as accorded by the Dutch society of pathology (`www.federa.org`). The samples were handled in a coded (pseudonymised) fashion according to the procedures as accorded by the LUMC ethical board.

Case ID	Age/Sex	Location	Multifocal regional spread	Treatment	Follow-up (month)	Break-Apart FOS (FISH)	RT-PCR
L3933[a,b]	F/42	Medial cuneiform bone, intermediate cuneiform bone, base metatarsal 1 and 2	Yes	Amputation	23, NED	Positive	*FOS-MBNL1*
L3141[b]	F/60	Metatarsal 4, metatarsal 2	Yes	Curettage, followed by amputation after relapse. Radiotherapy	73, NED	Positive	*FOS-VIM*
L4065[b]	M/50	Navicular bone, medial cuneiform bone, intermediate cuneiform bone, metatarsal 1	Yes	Amputation	14, NED	Not scorable	*FOS-lincRNA*
L3140	F/45	Vertebra T7	No	Vertebrectomy	63, NED	Not scorable	No
L3142	M/42	Femur diaphysis	No	Resection, radiotherapy	20, NED	Positive	No
L3151	M/33	Distal tibia, cuboid, cuneiform 3	Yes	Curettage	19, NED	Not scorable	No
L3153	M/83	Proximal tibia, distal tibia, fibula	Yes	Curettage, radiotherapy	72, NED	Not scorable	No
L3154	M/41	Metacarpal 2	No	Curettage	175, NED	Positive	No
L3157	M/40	Tibia diaphysis, proximal tibia, femur diaphysis	Yes	Knee disarticulation curettage, radiotherapy	114, NED	Not scorable	No
L3160	M/28	Proximal tibia	No	Curettage	36, NED	Negative	No
L3336	F/29	Metatarsal 1	No	Curettage	15, NED	Negative	No

Table 3.1: Clinical Features of Epithelioid Hemangioma Cases. [a]Index case that was used for the COBRA-FISH. [b]Cases that were transcriptome sequenced. NED: no evidence of disease; NA: not available.

3.3.2 Combined binary ratio labeling with multiple Fluorescence In Situ Hybridization (COBRA-FISH)

The tumor sample L3933 was obtained immediately after surgery and metaphase slides were prepared as described before (16). COBRA-FISH was performed as described by our group (16, 17).

3.3.3 Fluorescence In Situ Hybridization

FISH mapping using BAC clones selected from the 1MB clone set from the Welcome Trust, Sanger Institute (supplementary data 1 available online) were used to narrow down the translocation breakpoints in case L3933. Later, clones flanking the FOS locus were selected. Proximal and distal to *FOS*, BAC clones RP11-173A8 pooled with RP11-316E14 and RP11-361H10 pooled with RP11-368K8 were selected to detect rearrangements, respectively. DNA was extracted from the BAC clones using the High Pure Plasmid isolation kit (Roche, Woerden, The Netherlands). The two-color FISH was performed by labeling the probes with either biotin-11-dUTP or digoxigenin-11-dUTP (Roche, Woerden, The Netherlands) using a nick translation labeling reaction (18).

A two-color FISH for *FOS* break-apart (translocation) detection was performed on all cases. Four micrometer paraffin slides were prepared as described before and the labeled probe and the slides were denatured simultaneously at 80°C for 10 min. Thereafter slides were hybridized in a moist chamber overnight at 37°C. Posthybridization washing steps and fluorescent detection of probes were performed as described earlier (18). Slides were scanned using the Pannoramic MIDI scanner (3DHistech, Budapest, Hungary). Tumor areas were selected based on the hematoxylin and eosin stained slides and scored using Pannoramic Viewer software (3DHistech, Budapest, Hungary) by counting 100 nuclei. Cases were considered positive for a break when >20% of the nuclei showed a break-apart signal. Slides were scored by one observer (DGPIJ) and the conclusion was confirmed by a pathologist (JVMGB).

3.3.4 RNA sequencing using transcriptome sequencing

RNA was extracted from samples L3141, L3393, and L4065 for RNA sequencing. The samples were collected after surgery and stored at -80°C. From each sample 15, 20 μm slides were cut for RNA isolation. TRIzol (Life technologies, Carlsbad) was added to the cut tissue sections. The nucleotides were extracted from the mixture using chloroform and the content was precipitated using 2-propanol. The total nucleotides were washed using 75% ethanol and resuspended in Milli-Q water. An additional RNA purification step was included using the RNeasy Mini kit (Qiagen, Venlo, The Netherlands) according to the

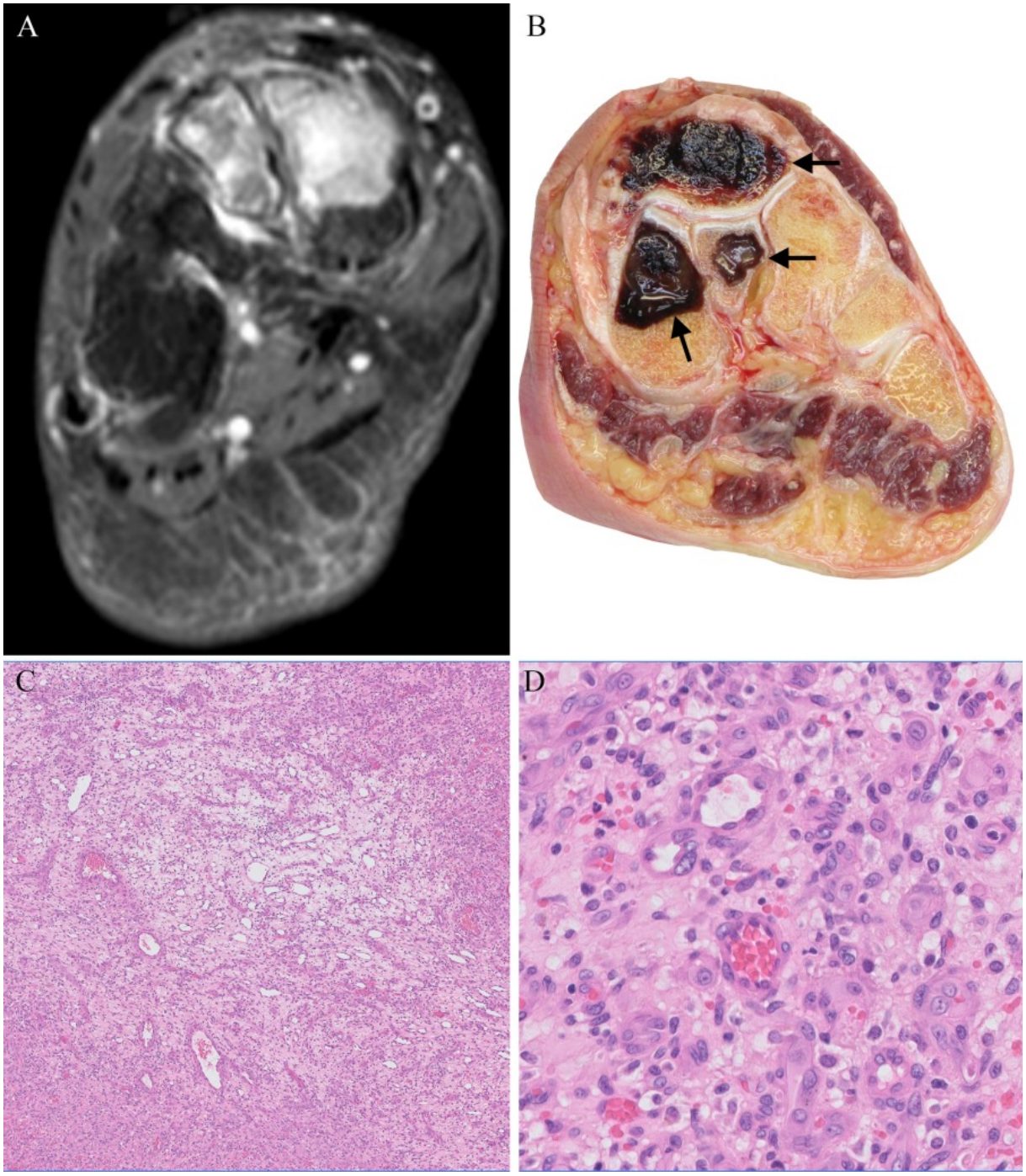

Figure 3.1: Epithelioid hemangioma case L4065 displaying multifocal regional spread revealing identical translocations in all separate tumors. (a) MRI image of multiple lesions in the foot. (b) Macroscopical image, at the same plane as the MRI, of the foot showing involvement of three separate tarsal bones (indicated by arrows). (c) H&E staining demonstrating vasoformative areas admixed with spindled and hemorrhagic areas at low power view. (d) High power view shows epithelioid cells lining vascular channels.

manufacturers protocol. The total RNA was send to BGI (Hong Kong) for sequencing with the HiSeq2000 platform (Illumina, San Diego).

3.3.5 RNA sequencing analysis with Defuse

An in-house pipeline was used to align the sequenced reads to the hg19 reference genome (`http://genome.ucsc.edu`) and analyze the data for SNVs. Sequence alignment was performed with TopHat2 (v2.0.13) aligning to the hg19 (`http://genome.ucsc.edu/`) and hg38 (`http://genome.ucsc.edu/`). SNVs were called with VarScan (v2.3.7). Annovar was used to annotate and filter the detected variants using the genomicSuperDups (`http://genome.ucsc.edu/`), snp138 (`http://genome.ucsc.edu/`) 1000 Genomes (`http://www.1000genomes.org/`), Exome Sequencing Project (`http://evs.gs.washington.edu/EVS/`), and the LJB23 nonsynonymous variant annotations (v2.3). Fusion detection was performed with Defuse (v0.6.2) aligning to the hg19 (`http://genome.ucsc.edu/`) and filtering with the repeats library from UCSC (`http://genome.ucsc.edu/`). Detected fusions were sorted according to fusion spanning reads.

3.3.6 RT-PCR

Total RNA was isolated from 10 frozen epithelioid hemangioma samples according to the protocol described above. cDNA was made using a mixture of RNasin, 5x RT-buffer, oligodT, random primer, dNTP's, and AMV-RT enzyme (Promega, Madison), which was added to the total RNA after denaturing the RNA for 15 min at 60°C and placing it on ice. The reverse transcriptase reaction was performed at 42°C for 1 hr. Then the enzyme was inactivated by heating the mix to 65°C for 15 min. Primers were designed for the fusions that were identified with Defuse. Primers for *FOS-MBNL1*, *FOS-VIM*, and *FOS-linc*RNA(RP11-326N17.1), were designed using Primer3 (v0.4.0). For *FOS-VIM* the forward primer 5'-GAGAAAAGGAGAATCCGAAGG-3' and reverse primer 5'-ATCTTCCGCTAGCAAGATGC-3' were used. For *FOS-MBNL1* the forward primer 5'-GAGAAAAGGAGAATCCGAAGG-3' and reverse primer 5'-TCCATAAGACGTGTGGG-TGT-3' were used. For *FOS-lincRNA*(RP11-326N17.1) the forward primer 5'-GAGAAAA-GGAGAATCCGAAGG-3' and the reverse primer 5'- GAAAATCTGAGCTGTAACCAAGC-3' were used. To compare wild-type *FOS* expression with the expression of the fusion genes primers were also made for the normal exon 4 of *FOS*. The forward primer 5'-GAGAAAAGGAGAATCCGAAGG-3' and reverse primer 5'-GTCAGAGGAAGGCTCAT-TGC-3' were used. RT-PCR was performed using the CFX touch 96 (BIO-RAD, Hercules). Primers were added to SYBR Green I (Life technologies, Carlsbad) and cDNA. RT-PCR ran at 55°C for 40 cycles with a 40 sec elongation time at 72°C. Sanger sequenc-

ing of the PCR product was performed by the LGTC (Leiden, The Netherlands) and the sequences were analyzed using Chromas (v2.1.1).

3.4 Results

3.4.1 A balanced t(3;14) and the approximate location for a translocation is determined

Using COBRA-FISH, we identified a balanced translocation 46,XX,t(3;14) in L3933 (figure 3.2). The approximate location of the translocation breakpoints was determined using BAC clones. Annealing locations for the BAC clones on the L3933 case are shown in supplementary data 1 available online. The break on chromosome 3 was between nt 151,839,044 and 152,021,576. The break on chromosome 14 was between nt 75,518,664 and 76,145,087.

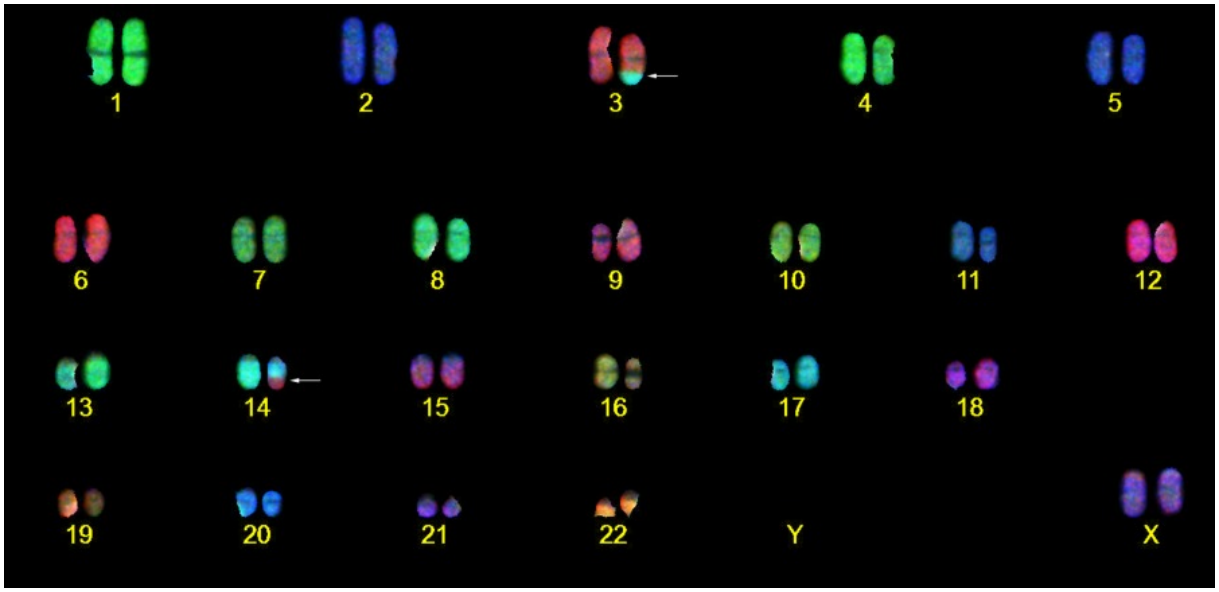

Figure 3.2: COBRA-FISH identifies a balanced 46,XX,t(3;14) translocation. Arrowheads are indicating the translocated chromosomes.

3.4.2 Three fusions involving *FOS* were identified

In index case L3933, Defuse identified a *FOS-MBNL1* translocation. *FOS* starts at position 75,745,477 on chromosome 14, matching to the fusion location that was identified using COBRA-FISH. *MBNL1* is located on chromosome 3 and starts at position 151,961,617 which matched to the expected location from the COBRA-FISH. In addition, Defuse identified fusions involving *FOS* in the two additional cases: L3141 had a *FOS-VIM* fusion

and L4065 had a *FOS-lincRNA* (RP11-326N17.1). All fusions were validated by RT-PCR (figure 3.3). In all three cases, the fusion-breakpoint in *FOS* is in exon 4. In the index case (L3933) nt position c.858 in exon 4 of *FOS* was fused to intron 2 of *MBNL1*, leading immediately to a stop codon at translation (figure 3.3a and GenBank accession number: KP790137). At the protein level this would lead to a truncation of the last 95 C terminal amino acids of the FOS protein. In case L3141 the break in *FOS* occurred at c.828 in exon 4 fused to the reverse complementary strand downstream of *VIM*. In the predicted fusion protein FOS would gain an additional (scrambled) 13 amino acids at the C terminal end before there is a stop codon (GenBank accession number: KP790138). In the case of L4065 the fusion occurred at c.806 in exon 4, where *FOS* was fused to a long non-coding RNA (RP11-326N17.1). FOS would gain an additional ten scrambled amino acids before a stop codon is encountered (GenBank accession number: KP790139). Therefore, in all three cases approximately 100 amino acids would be lost at the C terminal of the FOS protein, with loss of the transactivation domain (TAD) of *FOS*.

We sought for recurrent translocation events in our panel of epithelioid hemangioma samples performing an RT-PCR in the remaining 7 cases using all three translocation combinations using the index cases as positive controls; however, a recurrent fusion product was not detected in any of these cases.

Since truncation could also be caused by point mutation of the *FOS* gene, we examined exon 4 of *FOS* using RT-PCR and Sanger sequencing. No mutations were found in any of the 11 cases for which frozen material was available.

3.4.3 Cases with multifocal regional spread display identical fusion products in different Foci

For index case L3933 RNA was available from six separate tumors and for case L4065 there was RNA from three separate tumors. RT-PCR was performed on all tumor locations for the three identified fusions and the products were Sanger sequenced. None of the cases were positive for the *FOS-VIM* fusion. In the index case all separate tumors were positive for identical *FOS-MBNL1* fusions and in L4065 all separate tumors were positive for identical *FOS-lincRNA* (RP11-326N17.1), suggesting that the separately located tumors within one patient are derived from one single clone. Using FISH it was clear that the normal cells surrounding the tumor did not carry the translocation, excluding the possibility of a germline translocation.

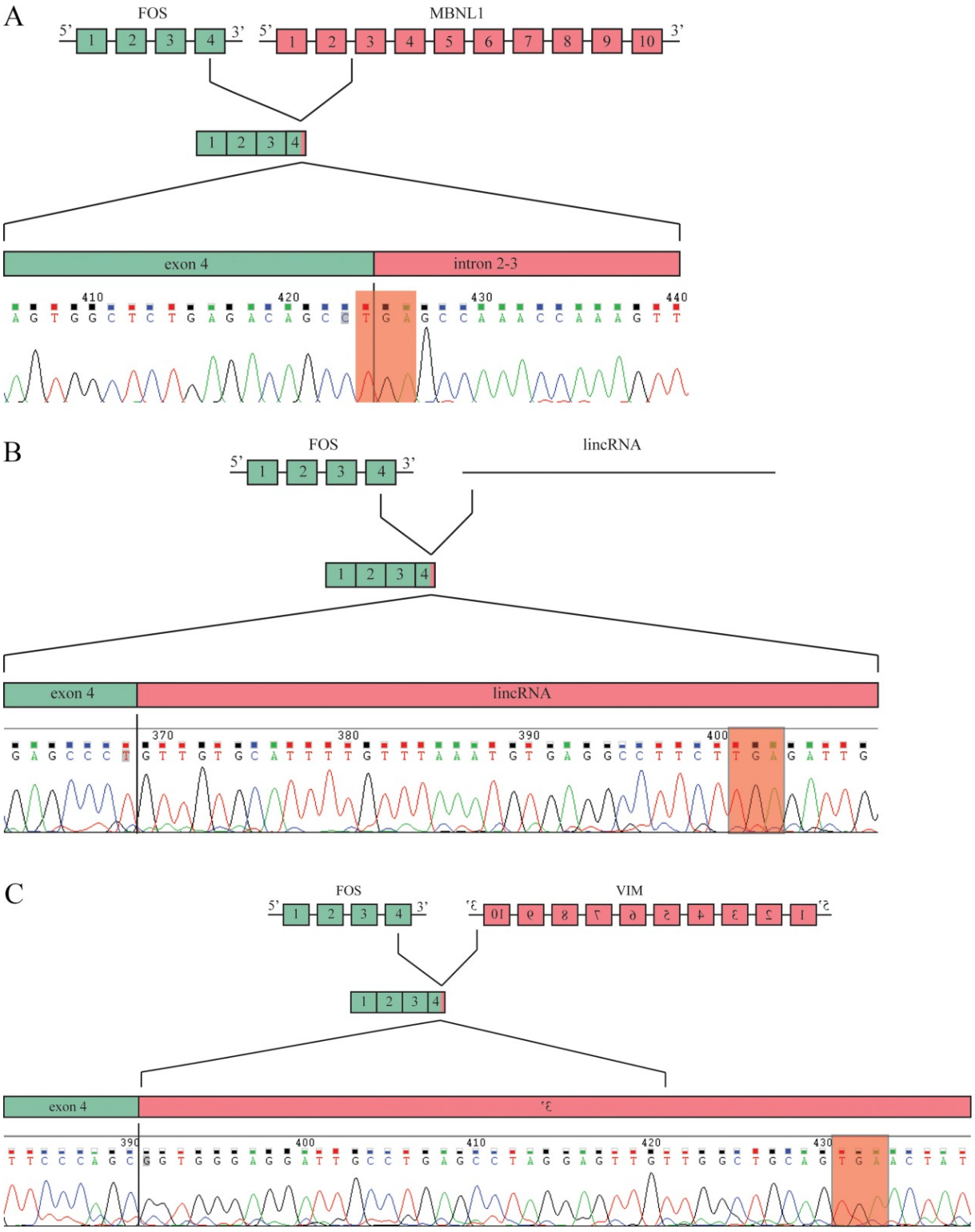

Figure 3.3: (a) The fusion product between *FOS* and *MBNL1* in case L3933. *FOS* gains a stop codon directly at the site of the translocation truncating the gene. (b) The fusion between *FOS* and *lincRNA* (RP11-326N17.1) in case L4065 resulting in a stop codon. (c) The *FOS-VIM* fusion in case L3141. *FOS* fuses to the reverse strand of *VIM* but gains a stop codon. Stop codons are highlighted in red.

3.4.4 A recurrent FOS break is present in 5/7 samples

As no recurrent translocations were detected using RT-PCR, interphase FISH analysis was performed to identify *FOS* rearrangement in the other cases. Five out of seven cases had a break-apart of *FOS* of which four out of six showed a scorable break-apart signal in the *FOS* locus (figure 3.4). Five cases could not be scored, including case L4065 that was found to have a fusion by transcriptome sequencing and RT-PCR.

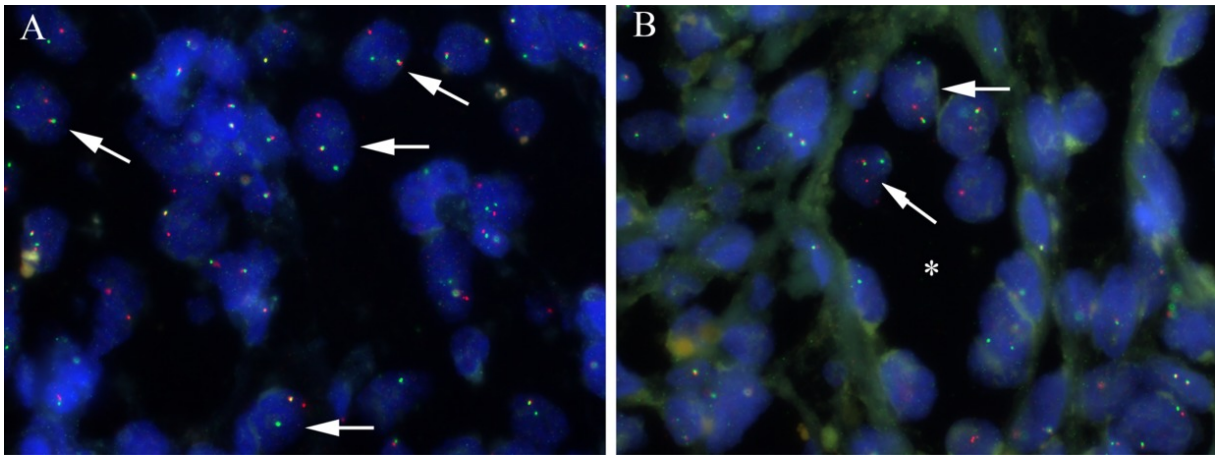

Figure 3.4: *FOS* break events. (a) Case L3142 showing four cells with a split signal (arrows). (b) Case L3154 shows two cells with a split signal (arrows). Both cases show a split and a colocalized signal in cells lining the vascular channel (star). The surrounding cells show only colocalized signals.

3.5 Discussion

While usually translocations in mesenchymal tumors lead to tumorigenesis by the creation of a chimeric transcription factor (deregulating transcription), or lead to upregulation of expression of a specific (onco) gene by promotor swap (deregulating transcription control) (19), we here report an uncommon mechanism in which a balanced translocation leads to truncation of a specific protein. We observed translocations involving the *FOS* gene with various partners in three epithelioid hemangiomas using transcriptome sequencing. Involvement of the *FOS* gene in bone and soft tissue epithelioid hemangioma was also very recently presented by Antonescu et al in an abstract (20). Intriguingly, based on the sequence it can be predicted that none of the fusion genes lead to an extended translation and formation of a chimeric protein. Instead, the translocation leads to a transcribed chimeric RNA with an early stop codon that may result in truncation of the FOS protein at translation.

Involvement of *FOS* by fusion events seems to be a highly specific and driving event in

epithelioid hemangioma. Complex genomic rearrangements were not detected in our index case using COBRA FISH based karyotyping, indicating that the balanced translocation might be a sole event. Also, transcriptome analysis of the three cases revealed no other recurrent mutations. Moreover, we observed *FOS* rearrangement by using split-apart FISH probe sets in two additional cases. Thus, in total, *FOS* rearrangement was found in five out of seven epithelioid hemangiomas of bone. Interestingly, none of the detected fusion events were found to be recurrent, indicating that in these two additional cases, yet other, novel fusion partners are involved. Since the introduction of a stop codon could also occur due to point mutations or small in/dels we sequenced exon 4 of *FOS* in 11 cases including the two cases without *FOS* rearrangements, without finding any mutations.

The diagnosis of vascular tumors of bone has been difficult, as there is considerable histomorphological overlap and immunohistochemical markers that can help in the distinction are lacking. The recent elucidation of *WWTR1-CAMTA1* and *YAP1-TFE3* fusions in epithelioid hemangioendothelioma has provided novel molecular tools that can help in the classification (14, 21, 22). Recently, a new translocation was identified involving a fusion between *ZFP36* and *FOSB* in a subset of epithelioid hemangiomas with atypical histological features (15). Also, for pseudomyogenic hemangioendothelioma, a recently described rare vascular tumor that also can occur in bone, a *SERPINE1-FOSB* fusion was described leading to upregulation of *FOSB* (23).

Approximately 18-25% of epithelioid hemangiomas demonstrate multifocal regional spread (7, 14), which was also seen in six of our cases. In the two cases for which we elucidated the exact fusion product using transcriptome sequencing, we could demonstrate using RT-PCR that in separate tumors, affecting different bones, an identical fusion product was present. Similar to our observations, in multifocal epithelioid hemangioendothelioma of the liver, identical *WWTR1-CAMTA1* fusions could be identified in the different foci (12). Our results indicate that also in epithelioid hemangioma the separate tumours affecting multiple bones as well as soft tissue are of monoclonal origin. Moreover, our FISH results excluded that the translocation occurs in the germline. Therefore, we may conclude that germline predisposition or a "field-effect" predisposing to the development of multiple independent neoplastic lesions in multiple adjacent bones is highly unlikely. Instead of the generally used "metastasis", we prefer the term "multifocal regional spread" as the multiple foci represent local spread of a single neoplastic clone to adjacent bones and soft tissue.

The predicted loss of approximately 100 amino acids at the C terminal region of the FOS protein results in the loss of the TAD. With primers covering the exon 4 of *FOS* we performed RT-PCR showing a substantial expression of the wild-type *FOS* (with average Ct value of normal *FOS* = 30, for fusions = 28, data not shown) in all cases,

indicating that the translocation does not lead to strong decreased expression of the intact allele. The in silico predicted, truncated FOS protein shows a high structural similarity to FOSL1, which also lacks the TAD (figure 3.5). FOS and FOSB are part of the FOS family of proteins, which also includes FOSL1 (also known as FRA-1) and FOSL2 (also now as FRA-2). All the members of the FOS family are involved in forming the Activator Protein-1 (AP-1) protein. The canonical AP-1 complex consists of FOS and JUN protein heterodimer, but other variants involving members of the FOS and JUN family of transcription factors have been described to be involved in the heterodimer as well, because of their structural similarities (24). FOSL1 knockdown in endothelial cells resulted in a decrease in angiogenesis through upregulation of the aVβ3 receptor, which is an important regulator of angiogenesis (25). It was shown that FOSL1 correlated with upregulation of adhesion proteins such as CD44 and integrin α5 resulting in an increase in adhesion (26). This is in contrast to endothelial cells where FOSL1 downregulates integrins, illustrating the different tissue-specific functions of FOSL1.

In models where *FOS* was knocked down, it was shown that many of the functions of FOS were taken over by FOSL1, although for some target genes FOSL1 fails to induce expression, indicating FOSL1 is not a full replacement for FOS (27). Furthermore, the activation pattern of FOSL1 and FOS is different. It was shown that by stimulation of fibroblasts by serum FOS and FOSB are rapidly and transiently induced whereas FOSL1 and FOSL2 are expressed in a more delayed and stable pattern (28, 29). In ER-positive breast cancer, patients with high FOSL1 expression showed significantly shorter survival and higher rates of lung metastasis. Furthermore, it was shown that fibroblastoid cells, which did not express FOSL1, transfection with *FOSL1* led to a strong enhancement of mobility in the cell line (30). It is tempting to speculate that these functions of FOSL1 may underlie the multifocal regional spread of epithelioid hemangioma of bone.

In conclusion, we identified rearrangement of FOS with various non-recurrent fusion partners in five out of seven classic epithelioid hemangiomas of bone. Detection of FOS rearrangement may therefore be a useful diagnostic tool to assist in the often-difficult differential diagnosis of vascular tumors of bone. In silico prediction shows that the translocations cause truncation of the FOS protein, with loss of the TAD, which is thereby a novel mechanism involved in tumorigenesis, which requires further studies.

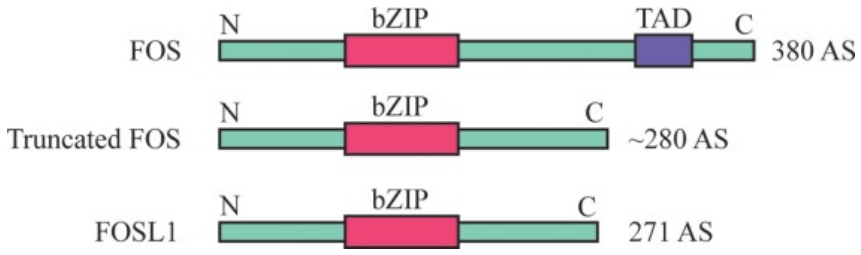

Figure 3.5: The fusions are predicted to result in the loss of 100 amino acids from FOS. This results in the loss of the TAD. The truncated FOS shows a large similarity in structure with FOSL1, which is also part of the FOS family of proteins.

Bibliography

[1] Rosenberg Ae BJ. Epithelioid haemangioma. In: Fletcher Cd BJAHPCWMF, editor. WHO Classification of Tumours of Soft Tissue and Bone. Lyon: IARC; 2013. p. 333–4.

[2] Nielsen GP, Srivastava A, Kattapuram S, Deshpande V, O'Connell JX, Mangham CD, et al. Epithelioid hemangioma of bone revisited: A study of 50 cases. American Journal of Surgical Pathology. 2009;33(2):270–277. doi:10.1097/PAS.0b013e31817f6d51.

[3] Fletcher CDM, Bridge JA, Hogendoorn P, Mertens F. Vascular tumours. Lyon: IARC; 2013.

[4] Errani C, Zhang L, Panicek DM, Healey JH, Antonescu CR. Epithelioid hemangioma of bone and soft tissue: A reappraisal of a controversial entity. Clinical Orthopaedics and Related Research. 2012;470(5):1498–1506. doi:10.1007/s11999-011-2070-0.

[5] Verbeke SLJ, Bovée JVMG. Primary vascular tumors of bone: A spectrum of entities? International Journal of Clinical and Experimental Pathology. 2011;4(6):541–551.

[6] Unni KK, Ivins JC, Beabout JW, Dahlin DC. Hemangioma, hemangiopericytoma, and hemangioendothelioma (angiosarcoma) of bone. Cancer. 1971;27(6):1403–1414. doi:10.1002/1097-0142(197106)27:6<1403::AID-CNCR2820270621>3.0.CO;2-6.

[7] Campanacci M, Boriani S, Giunti A. Hemangioendothelioma of bone: A study of 29 cases. Cancer. 1980;46(4):804–814. doi:10.1002/1097-0142(19800815)46:4<804::AID-CNCR2820460427>3.0.CO;2-1.

[8] Dorfman H, Czerniak B. Vascular lesions. Bone Tumors. 1998; p. 1:729–814.

[9] Wenger DE, Wold LE. Benign vascular lesions of bone: radiologic and pathologic features. Skeletal Radiol. 2000;29(2):63–74.

[10] Evans HL, Raymond AK, Ayala AG. Vascular tumors of bone: A study of 17 cases other than ordinary hemangioma, with an evaluation of the relationship of hemangioendothelioma of bone to epithelioid hemangioma, epithelioid hemangioendothelioma, and high-grade angiosarcoma. Human Pathology. 2003;34(7):680–689. doi:10.1016/S0046-8177(03)00249-1.

[11] Bruder E, Perez-Atayde AR, Jundt G, Alomari AI, Rischewski J, Fishman SJ, et al. Vascular lesions of bone in children, adolescents, and young adults. A clinicopathologic reappraisal and application of the ISSVA classification. Virchows Archiv. 2009;454(2):161–179. doi:10.1007/s00428-008-0709-3.

[12] Errani C, Zhang L, Sung YS, Hajdu M, Singer S, Maki RG, et al. A novel WWTR1-CAMTA1 gene fusion is a consistent abnormality in epithelioid hemangioendothelioma of different anatomic sites. Genes Chromosomes and Cancer. 2011;50(8):644–653. doi:10.1002/gcc.20886.

[13] Tanas MR, Ma S, Jadaan FO, Ng CK, Weigelt B, Reis-Filho JS, et al. Mechanism of action of a WWTR1(TAZ)-CAMTA1 fusion oncoprotein. Oncogene. 2016;35(7):929–938. doi:10.1038/onc.2015.148.

[14] Antonescu CR, Le Loarer F, Mosquera JM, Sboner A, Zhang L, Chen CL, et al. Novel YAP1-TFE3 fusion defines a distinct subset of epithelioid hemangioendothelioma. Genes Chromosomes and Cancer. 2013;52(8):775–784. doi:10.1002/gcc.22073.

[15] Antonescu CR, Chen HW, Zhang L, Sung YS, Panicek D, Agaram NP, et al. ZFP36-FOSB fusion defines a subset of epithelioid hemangioma with atypical features. Genes Chromosomes and Cancer. 2014;53(11):951–959. doi:10.1002/gcc.22206.

[16] Szuhai K, Tanke HJ. COBRA: Combined binary ratio labeling of nucleic-acid probes for multi-color fluorescence in situ hybridization karyotyping. Nature Protocols. 2006;1(1):264–275. doi:10.1038/nprot.2006.41.

[17] Szuhai K, Bezrookove V, Wiegant J, Vrolijk J, Dirks RW, Rosenberg C, et al. Simultaneous molecular karyotyping and mapping of viral DNA integration sites by 25-color COBRA-FISH. Genes Chromosomes and Cancer. 2000;28(1):92–97. doi:10.1002/(SICI)1098-2264(200005)28:1<92::AID-GCC11>3.0.CO;2-2.

[18] Rossi S, Szuhai K, Ijszenga M, Tanke HJ, Zanatta L, Sciot R, et al. EWSR1-CREB1 and EWSR1-ATF1 fusion genes in angiomatoid fibrous histiocytoma. Clinical Cancer Research. 2007;13(24):7322–7328. doi:10.1158/1078-0432.CCR-07-1744.

[19] Roukos V, Misteli T. The biogenesis of chromosome translocations. Nature Cell Biology. 2014;16(4):293–300. doi:10.1038/ncb2941.

[20] Huang S, Chen H, Zhang L, Sung Y, Dickson B, Krausz T, et al. Frequent FOS Gene Rearrangements in Epithelioid Hemangioma. Lab Invest. 2015;95:18A–19A.

[21] Tanas MR, Sboner A, Oliveira AM, Erickson-Johnson MR, Hespelt J, Hanwright PJ, et al. Identification of a disease-defining gene fusion in epithelioid hemangioendothelioma. Science Translational Medicine. 2011;3(98):98ra82–98ra82. doi:10.1126/scitranslmed.3002409.

[22] Errani C, Sung YS, Zhang L, Healey JH, Antonescu CR. Monoclonality of multifocal epithelioid hemangioendothelioma of the liver by analysis of WWTR1-CAMTA1 breakpoints. Cancer Genetics. 2012;205(1-2):12–17. doi:10.1016/j.cancergen.2011.10.008.

[23] Walther C, Tayebwa J, Lilljebjörn H, Magnusson L, Nilsson J, Von Steyern FV, et al. A novel SERPINE1-FOSB fusion gene results in transcriptional up-regulation of FOSB in pseudomyogenic haemangioendothelioma. Journal of Pathology. 2014;232(5):534–540. doi:10.1002/path.4322.

[24] Hess J. AP-1 subunits: quarrel and harmony among siblings. Journal of Cell Science. 2004;117(25):5965–5973. doi:10.1242/jcs.01589.

[25] Galvagni F, Orlandini M, Oliviero S. Role of the AP-1 transcription factor FOSL1 in endothelial cell adhesion and migration. Cell Adhesion and Migration. 2013;7(5):408–411. doi:10.4161/cam.25894.

[26] Oliveira-Ferrer L, K??rschner M, Labitzky V, Wicklein D, M??ller V, L??ers G, et al. Prognostic impact of transcription factor Fra-1 in ER-positive breast cancer: contribution to a metastatic phenotype through modulation of tumor cell adhesive properties. Journal of Cancer Research and Clinical Oncology. 2015;141(10):1715–1726. doi:10.1007/s00432-015-1925-2.

[27] Fleischmann A, Hafezi F, Elliott C, Remé CE, Rüther U, Wagner EF. Fra-1 replaces c-Fos-dependent functions in mice. Genes and Development. 2000;14(21):2695–2700. doi:10.1101/gad.187900.

[28] Milde-Langosch K. The Fos family of transcription factors and their role in tumourigenesis. European Journal of Cancer. 2005;41(16):2449–2461. doi:10.1016/j.ejca.2005.08.008.

[29] Chalmers CJ, Gilley R, March HN, Balmanno K, Cook SJ. The duration of ERK1/2 activity determines the activation of c-Fos and Fra-1 and the composition and quantitative transcriptional output of AP-1. Cellular Signalling. 2007;19(4):695–704. doi:10.1016/j.cellsig.2006.09.001.

[30] Tkach V, Tulchinsky E, Lukanidin E, Vinson C, Bock E, Berezin V. Role of the Fos family members, c-Fos, Fra-1 and Fra-2, in the regulation of cell motility. Oncogene. 2003;22(32):5045–5054. doi:10.1038/sj.onc.1206570.